FeO(OH)@C-Catalyzed Selective Hydrazine Substitution of *p*-Nitro-Aryl Fluorides and their Application for the Synthesis of Phthalazinones

Dingzhong Li,[a] Wensheng Zhang,[a] Longzhi Zhu,*[b] Shuang-Feng Yin,[a] Nobuaki Kambe,[a] and Renhua Qiu*[a]

An efficient hydrazine substitution of *p*-nitro-aryl fluorides with hydrazine hydrates catalyzed by FeO(OH)@C nanoparticles is described. This hydrazine substitutions of *p*-nitro-aryl fluorides bearing electron-withdrawing groups proceeded efficiently with high yield and selectivity. Similarly, hydrogenations of *p*-nitro- aryl fluorides containing electron-donating groups also smoothly proceeded under mild conditions. Furthermore, with these prepared aryl hydrazines, some phthalazinones, interesting as potential structures for pharmaceuticals, have successfully been synthesized in high yields.

Introduction

Arylhydrazines are an important structural motif in agrochemicals,[1] pharmaceuticals,[2] and functional materials.[3] Some heterocycles such as indoles,[4] arylpyrazoles/ pyrazolenes,[5] aryltriazoles,[6] indazoles,[7] and phthalazinones[8] can also be efficiently generated from arylhydrazines, especially in the construction of the core structures of numerous pharmaceuticals, such as cancer inhibitors,[9] anti-hypertensive,[10] and anti-asthmatic pharmaceuticals[11] (Figure 1).

Therefore, it is of great importance to develop efficient and convenient methods to obtain arylhydrazines. The nucleophilic substitution of aryl halides with hydrazine hydrate[12] and the diazotization of anilines followed by reduction of the diazonium salt by employing the toxic system SnCl$_2$/HCl[13] are two classical strategies for the synthesis of arylhydrazines. However, the above-mentioned methods have some disadvantages. For example, the nucleophilic hydrazine substitution pathway typically proceeds at high temperatures, resulting in increasing amounts of impurities. The aniline diazotization/reduction path-
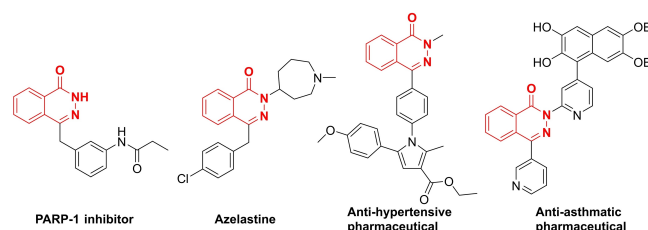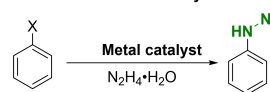

Figure 1. Structures of pharmaceuticals containing phthalazinone skeletons.

way suffers from harsh reaction conditions, generating unstable and explosive diazonium intermediates, and from producing large amounts of waste.

In recent years, metal-catalyzed C—N cross-coupling reactions of aryl halides and hydrazine hydrates attracted much attention for the synthesis of arylhydrazines due to the advantages of high yield, selectivity, and generally more environmentally friendly features (Scheme 1A).[14] For example,
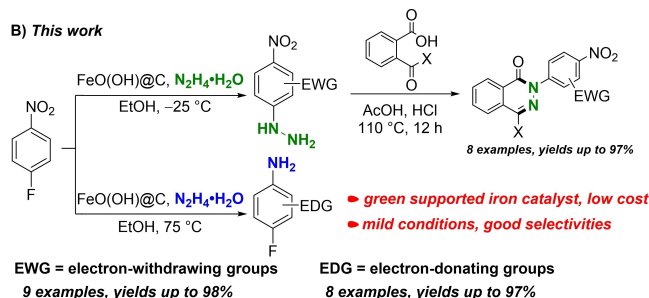
[a] D. Li, W. Zhang, Prof. Dr. S.-F. Yin, Prof. Dr. N. Kambe, Prof. Dr. R. Qiu
State Key Laboratory of Chemo/Biosensing and Chemometrics, College of Chemistry and Chemical Engineering
Hunan University
Changsha, 410082 (P. R. China)
E-mail: renhuaqiu1@hnu.edu.cn
[b] Dr. L. Zhu
Center for Biomedical Optics and Photonics (CBOP) & College of Physics and Optoelectronic Engineering, Key Lab of Optoelectronics Devices and systems of Ministry of Education/Guangdong Province
Shenzhen University
Shenzhen 518060 (P. R. China)
E-mail: zhulongzhi@hnu.edu.cn

Scheme 1. Approaches for the metal-catalyzed hydrazine substitution of halogenated aromatics.

Hartwig et al. reported a Pd-catalyzed cross-coupling reaction of hydrazine hydrates and (hetero)aryl halides to form aryl hydrazines with high yields with only low catalyst loading.[14d] However, the high costs of the precious metals and residual traces of heavy metal, generally disfavored especially in medicinal chemistry, are still problematic. Therefore, the development of green and efficient methods for the synthesis of aromatic hydrazines using C–N cross-coupling is of great value in organic synthesis and still highly sought after.

Since iron is an abundant environmentally friendly, relatively non-toxic and inexpensive metal,[15] the choice of iron as a catalyst for aromatic hydrazine substitution has attracted our attention. To date, there was no report about iron-catalyzed C–N cross-coupling of aryl halides with hydrazine hydrates. Since hydrazine hydrate is a strong reductant, it can reduce transition metals to low-valent aggregates and may lower the catalytic activity. Preparing a supported heterogeneous catalyst and encapsulating the transition metal into pores and channels may solve this problem. Previously, we developed Cunninghamia lanceolata *(C. lanceolata)*-carbon-supported iron oxide hydroxide nanoparticles with good specific surface area and pore size distribution,[16] which we considered could potentially show good catalytic activity in the aromatic hydrazine substitution.
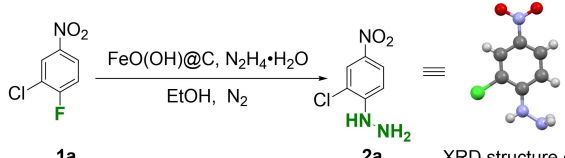
In this work, we report an efficient and selective synthesis of arylhydrazines catalyzed by heterogeneous *C. lanceolata*-carbon-supported iron oxide hydroxide FeO(OH)@C (Scheme 1B), as well as the high-yielding preparation of selected phthalazinones from the obtained aromatic hydrazines.

Results and Discussion

Initially, to evaluate the catalytic activity of the prepared FeO(OH)@C nanoparticles, we chose 3-chloro-4-fluoronitrobenzene (**1a**) and hydrazine hydrate as substrates to identify optimal reaction conditions. As shown in Table 1, we first optimized the reaction with regard to different catalyst loadings (entries 1–4). The target product was obtained with yields ranging from 48 to 92%, indicating good catalytic activity of the *C. lanceolata*-carbon-supported iron oxide hydroxide nanoparticles. Hence, we chose 50 mg of FeO(OH)@C nanoparticles/1 mol substrate (entry 3) for the following optimization. Next, we investigated the amount of hydrazine hydrate (entries 3, 5–7), and found 2.0 equiv. of hydrazine hydrate to be suitable. Then, the reaction temperature was also investigated. Lower temperatures are favored, while higher temperatures resulted in lower yields of the desired product **2a** (entries 8–10). Finally, we identified optimized reaction conditions for the hydrazine substitution as follow: **1a** (1 mmol), 80% hydrazine hydrate (2 equiv.), FeO(OH)@C nanoparticles (50 mg), EtOH (2.0 mL), −25°C (Table 1, entry 8, yield 96%). The structure of product **2a** was unambiguously confirmed by single-crystal X-ray analysis (Figure in Table 1).[17]

With this optimized reaction conditions in hand, we then explored the substrate scope with a series of *p*-nitro-aromatic fluorides bearing various kinds of functional groups. As shown

Table 1. Reaction condition optimization for the hydrazine substitution of *p*-nitro-aromatic fluorides.[a]

Entry	FeO(OH)@C [mg]	$N_2H_4 \cdot H_2O$ [equiv.]	Temperature [°C]	Yield [%]
1	20	2	rt	48
2	40	2	rt	82
3	50	2	rt	92
4	60	2	rt	92
5	50	1	rt	69
6	50	1.5	rt	80
7	50	2.5	rt	91
8	**50**	**2**	**−25**	**96**
9	50	2	0	93
10	50	2	50	68

[a] Reaction conditions: **1a** (1 mmol), 80% hydrazine hydrate (1–2.5 equiv.), FeO(OH)@C nanoparticles (20–60 mg), EtOH (2.0 mL), −25–50°C, 3 h; isolated yields.

in Scheme 2, the presence of one additional electron-withdrawing group (EWG), such as 2-Cl, 3-F, 3-CN, and 2-Br, on the the *p*-nitro-aromatic fluorides allowed the hydrazine substitution to proceed well with the desired products generated in high yields (**2a–2c**, **2g** in 96%, 96%, 94%, and 96% yield, respectively). When the *p*-nitro-aromatic fluorides contain two additional electron-withdrawing groups, the hydrazine substitution took place dominantly in *para*-position to the fluorine atom of the starting material, generating the corresponding products in good yields (**2d**, **2e**, **2f**, **2h** in 90%, 89%, 89% and 88% yield, respectively).
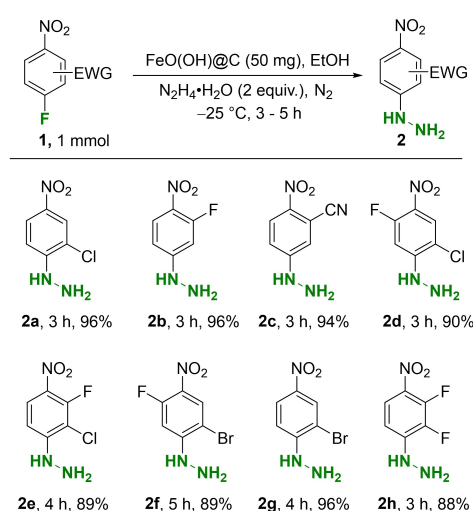
Scheme 2. Hydrazine substitution of *p*-nitro-aromatic fluorides catalyzed by FeO(OH)@C nanoparticles. Reaction conditions: **1** (1 mmol), 80% hydrazine hydrate (0.126 g, 2 mmol), EtOH (2 mL), FeO(OH)@C nanoparticles (50 mg), N_2, −25°C to rt, 3–5 h; isolated yield.

ChemistryOpen

Research Article
doi.org/10.1002/open.202200023

Chemistry Europe
European Chemical
Societies Publishing

To study the catalytic recyclability of the FeO(OH)@C nanoparticles, we used 3-chloro-4-fluoronitrobenzene (**1a**) as a substrate to react with hydrazine hydrate in the presence of recycled FeO(OH)@C under the previously optimized conditions. After the reaction was finished, and the catalyst had been filtered off and washed with water, the recycled FeO(OH)@C nanoparticle catalyst was dried overnight at 110 °C. Over three runs, product **2a** was obtained in 92–95% yield. We further-more checked the stability of the FeO(OH)@C nanoparticle catalyst by drying overnight at temperatures ranging from 100 to 180 °C. Again, product **2a** was obtained in 92–96% yield using the previously optimized conditions. These results show that the FeO(OH)@C nanoparticle catalyst has good recyclability and stability.

Interestingly, we found that products with amino groups, resulting from reduction of the nitro substituents, were obtained when *p*-nitro-aromatic fluorides containing electron-donating groups were employed as substrates (see Scheme 3). We observed that *p*-nitro-aromatic fluorides with an electron-donating group (EDG), such as dimethyl, methyl, methoxy and amino groups, provided high yields of the reduced products (**4a–4d**, **4g** in 94%, 96%, 97%, 90% and 93%, respectively). In addition, also a *p*-nitro-aromatic fluoride containing an hydroxyl group gave the corresponding product **4e** in a good 89% yield. When the *p*-nitro-aromatic fluoride without any EDGs was used, a moderate yield was observed (**4f** in 76% yield). Furthermore, we found that the 3-bromo-substituted *p*-nitro-aromatic fluoride provided the reduced amine product **4h** in 95% yield rather than undergoing hydrazine substitution.

As discussed and shown in Schemes 2 and 3, *p*-nitro-aromatic fluorides containing electron-withdrawing groups yielded hydrazine-substituted products, as electron-withdrawing groups can decrease the electron density of the aromatic nucleus, thus enhancing the leaving group ability of fluorine, promoting the hydrazine substitution. However, when the electron-withdrawing group is not strong enough to effectively decrease the electron density of the aryl motif and drive the

fluorine group to leave, hydrogenated amino products (**4h** for example) were formed, also helped by electron-donating groups, the electron-donating group through increasing the electron density of the aromatic core.

Phthalazinones are attractive diazabicyclo compounds due to their pharmaceutical bioactivity.[18] We were thus also interested in synthesizing phthalazinones using our developed hydrazine substitution method, which may be useful for the development of new pharmaceuticals. The synthesized aromatic hydrazines were selected as substrates to react with 2-(4-hydroxylbenzoyl)benzoic acid or 2-formylbenzoic acid to synthesize various kinds of phthalazinones. The hydrazine-substituted product **2a** and 2-formylbenzoic acid (**5a**) were used to optimize the reaction conditions (see Table 2). Firstly, we found that concentrated (conc.) HCl and conc. H_2SO_4 could efficiently drive the cyclization process with 1 equiv. of **5a** at 120 °C, and conc. HCl was the best (entries 1–3) acid choice. Further increasing the amount of 2-formylbenzoic acid (**5a**) did not significantly enhance the yield (entries 4–5). The amount of added conc. HCl was also investigated, and using 2.0 equiv. led to the best result (entries 6–8). We found that the reaction temperature could be lowered to 110 °C (entries 9–10), arriving at the following optimized conditions: **2a** (1 mmol), 2-formylbenzoic acid (1.1 equiv.), concentrated HCl (2 equiv.), HOAc (2.0 mL), 110 °C, 12 h (Table 2, entry 10, yield 97%).

After having defined optimal reaction conditions, we sought to explore the scope of the reaction with 2-(4-hydroxylbenzoyl)benzoic acids or 2-formylbenzoic acids, and various substituted phthalazinones were successfully obtained in high yields (**6a–6h** in 91–97% yields) (Scheme 4).

The following control experiments were performed to investigate a possible reaction mechanism (Scheme 5). Firstly, the yield did not decrease when 2,2,6,6-tetramethyl-1-piperidi-nyloxy (TEMPO) was added to the model reaction of **1a** with hydrazine hydrate, showing that the hydrazine substitution does likely not involve a free radical process (Scheme 5a). Secondly, we performed the model reaction using standard
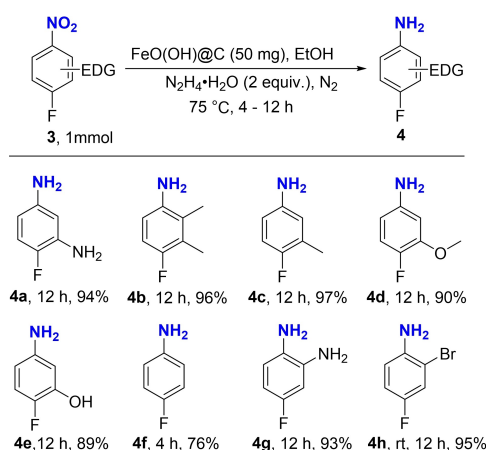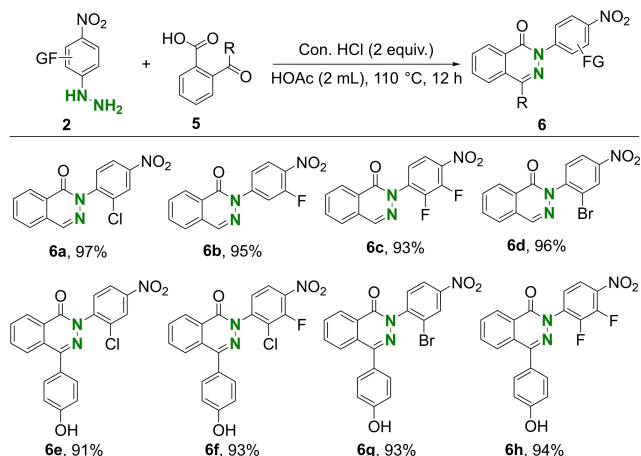
Scheme 3. Nitro hydrogenation of *p*-nitro-aromatic fluorides catalyzed by FeO(OH)@C nanoparticles. Reaction conditions: **3** (1 mmol), 80% hydrazine hydrate (0.126 g, 2 equiv.), 2 mL EtOH, FeO(OH)@C nanoparticles (50 mg), N_2, 75 °C, 4–12 h; isolated yield.
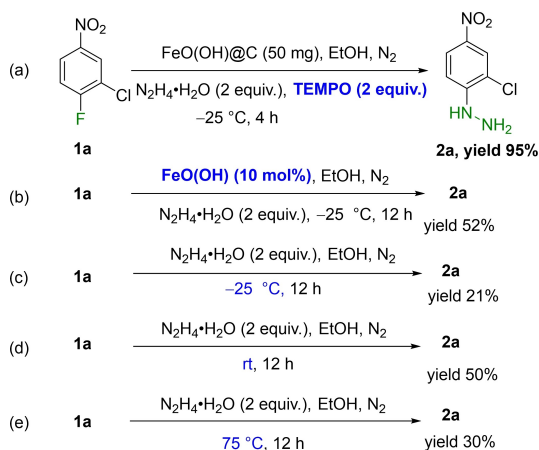
Table 2. Optimization of ring-closure conditions.[a]

Entry	**5a** (equiv.)	Acid (equiv.)	Temperature [°C]	Yield of **6a** [%]
1	1	Con. HCl, 2	120	92
2	1	Con. H_2SO_4, 2	120	86
3	1	–	120	55
4	1.1	Con. HCl, 2	120	94
5	1.2	Con. HCl, 2	120	95
6	1.1	Con. HCl, 1	120	91
7	1.1	Con. HCl, 1.5	120	92
8	1.1	Con. HCl, 2	120	93
9	1.1	Con. HCl, 2	100	91
10	1.1	Con. HCl, 2	110	97

[a] Reaction conditions: **2a** (1 mmol), 2-formylbenzoic acid (1–1.2 equiv.), concentrated HCl (1–2.5 equiv.) or H_2SO_4 (2 equiv.), HOAc (2.0 mL), 100–120 °C, 12 h; isolated yields.

ChemistryOpen

Research Article
doi.org/10.1002/open.202200023

**Chemistry
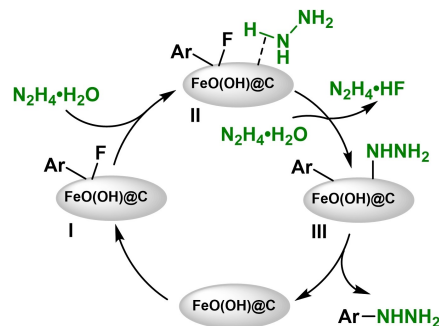Europe**
European Chemical
Societies Publishing

Scheme 4. Synthesis of phthalazinones using *p*-nitro-aromatic hydrazines. Reaction conditions: **2** (1 mmol), **5** (1.1 equiv.), concentrated HCl (2 equiv.), HOAc (2.0 mL), 110 °C, 12 h; isolated yields.

Scheme 5. Control experiments (TEMPO = (2,2,6,6-Tetramethylpiperidin-1-yl)oxyl).

Scheme 6. Possible mechanism.

After the dissociation of HF, which may be subsequently captured by hydrazine hydrate, intermediate **III** is formed. The final product is then obtained after an reductive elimination.

Conclusions

In summary, a simple and efficient protocol for the selective synthesis of aromatic hydrazines from *p*-nitro-aromatic fluorides is developed, catalyzed by *C. lanceolata* carbon-supported iron oxide nanoparticles. When *p*-nitro-aromatic fluorides bearing electron-withdrawing groups are reacted with hydrazine hydrates at low temperature, these substrates form produce hydrazine-substituted products. However, when *p*-nitro-aromatic fluorides contain electron-donating groups, reduction of the nitro group to yield amino-substituted products occurs. Followingly, selected phthalazinones have been successfully synthesized with high yields from the obtained aromatic hydrazines.

Experimental Section

General Information: All reagents and solvents were purchased from Leyan Reagent Co., Ltd. Industrial *C. lanceolata* carbon was purchased from Haixing Water Supply Materials (Gongyi) Co., Ltd. NMR spectra were recorded on a Bruker Avance 400 spectrometer operating at 400 MHz (^{1}H NMR), 101 MHz (^{13}C NMR) and 376 MHz (^{19}F NMR) in CDCl$_3$ or DMSO-d_6. All ^{1}H NMR, ^{13}C NMR and ^{19}F NMR chemical shifts were reported in ppm relative to internal references of CDCl$_3$ at 7.26 ppm, carbon resonance in CDCl$_3$ at 77.00 ppm, DMSO-d_6 at 2.5 ppm, carbon resonance in DMSO-d_6 at 39.95 ppm, respectively. The following abbreviations are used to describe peak patterns where appropriate: singlet, doublet (d), triplet (t), multiplet (m), broad resonances (br).

Process for the Preparation of Industrial *Cunninghamia lanceolata* Carbon-supported Iron Oxide Hydroxide Nanoparticles

The formation of industrial *C. lanceolata* carbon-supported iron oxide hydroxide catalyst particles was based on an established method.[16,21] To a solution of FeCl$_3$ (2.7 g FeCl$_3$·6H$_2$O dissolved in 30 mL of purified water) were added 12 g of industrial *C. lanceolata* carbon. Then, a 50% NaOH solution (1.0 g of NaOH dissolved in 1.0 mL of water) was added dropwise. The reactant was stirred at

conditions, that is, using non-carbon supported FeO(OH) and longer reaction times. In this case, the desired product **2a** was generated with only 52% yield (Scheme 5b), indicating the important role of the carbon supported. **1a** was also tested to react with hydrazine hydrate without our catalyst, the industrial *C. lanceolata* carbon-supported FeO(OH) nanoparticles, at elevated temperatures, which resulted in only 21–50% yield of **2a** (Scheme 5c–5e). The above-detailed control experiments clearly show that the prepared FeO(OH)@C particles can effectively catalyzed the hydrazine substitution, and both of the support and the metal are essential to the catalytic activity.

On the basic of previous literature[14d,19] and the control experiments, we propose a possible mechanism as shown in Scheme 6. First, the nitro aryl fluorides are absorbed on the surface of the *C. lanceolata* carbon-supported iron oxide, and the active species iron then inserts into the C–F bond to form intermediate **I**. In the next step, hydrazine hydrate coordinates. The N$_2$H$_4$ may form N$_2$H$_3^-$ and H$^+$ species on the surface of the nanoparticles,[20] leading to the generation of intermediate **II**.

ChemistryOpen

Research Article
doi.org/10.1002/open.202200023

Chemistry Europe
European Chemical
Societies Publishing

70 °C for about 1 h and cooled down to room temperature. The obtained black solid was filtered and washed with purified water 3 times, and dried overnight at 80 °C to obtain a black solid (10.5 g).

Procedure for the Hydrazine Substitution of *p*-Nitro-aromatic Fluorides

To a 10 mL glass reactor were added 1 mmol of a *p*-nitro-aromatic fluoride, 50 mg of *C. lanceolata* carbon-supported iron oxide hydroxide nanoparticles, and 2 mL of ethanol under an N_2 atmosphere. Then the temperature was cooled down to −25 °C, 80 % $N_2H_4 \cdot H_2O$ (0.126 g, 2 mmol) was added dropwise under an N_2 atmosphere. Next, the reaction mixture was stirred at this temperature for 3–5 h. After the reaction was finished, the catalyst was filtered off and washed with ethyl acetate. The solvent was removed in vacuo, and the target products (**2a**–**2h**) were purified by column chromatography or directly dried in vacuo.

Procedure for the Hydrogenation of *p*-Nitro-aromatic Fluorides

To a 10 mL glass reactor were added 1 mmol of a *p*-nitro-aromatic fluoride, 50 mg of *C. lanceolata* carbon-supported iron oxide hydroxide nanoparticles, 80 % $N_2H_4 \cdot H_2O$ (0.126 g, 2 mmol) and 2 mL of ethanol under an N_2 atmosphere. Then, the temperature was raised to 75 °C, and the reaction mixture was stirred at this temperature for 4–12 h. After the reaction was finished, the catalyst was filtered off and washed with ethyl acetate. The solvent was removed in vacuo, and the target products (**4a**–**4h**) were purified by column chromatography or directly dried in vacuo.

Procedure for the Synthesis of Phthalazinones

To a 10 mL glass reactor were added aromatic hydrazines (1 mmol), 2-(4-hydroxylbenzoyl)benzoic acid (262 mg, 1.1 mmol) or 2-formylbenzoic acid (165 mg, 1.1 mmol), 37 % conc. HCl (196 mg, 2 mmol) and HOAc (2 mL). Then, the temperature was raised to 110 °C, and the reaction mixture was stirred at this temperature for 12 h. After the reaction was finished, the mixture was added to 20 mL of water, and stirred for 0.5 h, after which the solid was filtered and washed with 10 mL of water and subsequently dried overnight at 80 °C to obtain the target phthalazinones.

Conflict of Interest

The authors declare no conflict of interest.

Data Availability Statement

Research data are not shared.

[1] a) T. Wang, X. S. Qing, C. Dai, Z. J. Su, C. D. Wang, *Org. Biomol. Chem.* **2018**, *16*, 2456–2463; b) F. Giornal, S. Pazenok, L. Rodefeld, N. Lui, J. P. Vors, F. R. Leroux, *J. Fluorine Chem.* **2013**, *152*, 2–11; c) J. B. Liu, H. P. Zhou, Y. Y. Peng, *Tetrahedron Lett.* **2014**, *55*, 2872–2875.

[2] a) P. Ertl, S. Jelfs, J. Mühlbacher, A. Schuffenhauer, P. Selzer, *J. Med. Chem.* **2006**, *49*, 4568–4573; b) C. Mauger, G. Mignani, *Adv. Synth. Catal.* **2005**, *347*, 773–782; c) K. Xu, T. Gilles, B. Breit, *Nat. Commun.* **2015**, *6*, 7616.

[3] a) M. Kempasiddaiah, V. Kandathil, R. B. Dateer, B. S. Sasidhar, S. A. Patil, *Transition Met. Chem.* **2021**, *46*, 273–281; b) S. Chang, L. L. Dong, H. Q. Song, B. Feng, *Org. Biomol. Chem.* **2018**, *16*, 3282–3288.

[4] a) Y. K. Lim, C. G. Cho, *Tetrahedron Lett.* **2004**, *45*, 1857; b) T. Matsuda, Y. Tomaru, *Tetrahedron Lett.* **2014**, *55*, 3302–3304.

[5] a) S. Fustero, M. Sánchez-Rosell, P. Barrio, A. Simón-Fuentes, *Chem. Rev.* **2011**, *111*, 6984–7034.

[6] a) A. Ilangovan, P. Sakthivel, P. Sakthivel, *Org. Chem. Front.* **2016**, *3*, 1680–1685; b) M. J. Kurth, M. M. Olmstead, M. J. Haddadin, *J. Org. Chem.* **2005**, *70*, 1060–1062; c) L. De Luca, G. Giacomell, S. Masala, A. Porcheddu, *J. Org. Chem.* **2003**, *68*, 4999–5001.

[7] I. Uriarte, F. Reviriego, C. Calabrese, J. Elguero, Z. Kisiel, I. Alkorta, E. J. Cocinero, *Chem. Eur. J.* **2019**, *25*, 10172–10178.

[8] M. M. Heravi, B. Baghernejad, H. A. Oskooie, F. F. Bamoharram, *Heterocycl. Commun.* **2008**, *14*, 375–384.

[9] a) P. M. Wood, L. W. L. Woo, J. R. Labrosse, M. N. Trusselle, S. Abbate, G. Longhi, E. Castiglioni, R. Lebon, A. Purohit, M. J. Reed, B. V. L. Potter, *J. Med. Chem.* **2008**, *51*, 4226–4238; b) B. I. Rini, B. Escudier, P. Tomczak, A. Kaprin, C. Szczylik, T. Ehutson, M. D. Michaelson, M. E. Gore, P. G. Rusakov, Y. C. Ou, H. Y. Lim, H. Uemura, J. Tarazi, D. Cella, C. Chen, R. Jmotzer, *Lancet* **2011**, *378*, 1931–1939; c) H. F. Qi, L. G. Chen, B. N. Liu, X. R. Wang, L. Long, D. K. Liu, *Bioorg. Med. Chem. Lett.* **2014**, *24*, 1108–1110; d) P. K. Parikh, M. D. Ghate, *Eur. J. Med. Chem.* **2018**, *143*, 1103–1138; e) H. W. Hsu, R. D. Necochea-Campion, V. Williams, P. J. Duerksen-Hughes, A. A. Simental Jr., R. L. Ferris, C. S. Chen, S. Mirshahidi, *Oral Oncol.* **2014**, *50*, 662–669; f) J. Cuzick, I. Sestak, J. F. Forbes, M. Dowsett, S. Cawthorn, R. E. Mansel, S. Loibl, B. Bonanni, D. G. Evans, A. Howell, *Lancet* **2020**, *395*, 117–122; g) M. G. Ferlin, D. Carta, R. Bortolozzi, R. Ghodsi, A. Chimento, V. Pezzi, S. Moro, N. Hanke, R. W. Hartmann, G. Basso, G. Viola, *J. Med. Chem.* **2013**, *56*, 7536–7551.

[10] M. A. MacLean, E. Diez-Cecilia, C. B. Lavery, M. A. Reed, Y. F. Wang, D. F. Weaver, M. Stradiotto, *Bioorg. Med. Chem. Lett.* **2016**, *26*, 100–104.

[11] Y. Yuan, Y. Yu, J. Qiao, P. Liu, B. Y. Yu, W. K. Zhang, H. L. Liu, H. He, Z. L. Huang, A. W. Lei, *Chem. Commun.* **2018**, *54*, 11471–11474.

[12] a) D. D. Liang, M. X. Wang, *J. Org. Chem.* **2018**, *83*, 3316–3324; b) D. D. Liang, M. X. Wang, *Org. Chem. Front.* **2017**, *4*, 1425–1529; N. Nebel, S. Strauch, S. Maschauer, R. Lasch, H. Rampp, S. K. Fehler, L. R. Bock, H. Huebner, P. Gmeiner, M. R. Heinrich, O. Prante, *ACS Omega* **2017**, *2*, 8649–9659.

[13] a) Y. T. Han, J. W. Jung, N. J. Kim, *Curr. Org. Chem.* **2017**, *21*, 1265–1291; b) S. Kotha, M. Saifuddin, V. R. Aswar, *Org. Biomol. Chem.* **2016**, *14*, 9868–9873; c) A. Tiwari, V. Tiwari, C. H. S. Venkataramana Madhavan, *Asian J. Chem.* **2011**, *23*, 1179–1182.

[14] a) A. Mata, D. N. Tran, U. Weigl, J. D. Williams, C. O. Kappe, *Chem. Commun.* **2020**, *56*, 14621–14624; b) J. M. Chen, Y. M. Zhang, W. Y. Hao, R. L. Zhang, F. Yi, *Tetrahedron.* **2013**, *69*, 613–617; c) R. J. Lundgren, M. Stradiotto, *Angew. Chem. Int. Ed.* **2010**, *49*, 8686–8690; *Angew. Chem.* **2010**, *122*, 8868–8872; d) J. Y. Wang, K. Choi, S. J. Zuend, K. Borate, H. Shinde, R. Goetz, J. F. Hartwig, *Angew. Chem. Int. Ed.* **2021**, *60*, 399–408; *Angew. Chem.* **2021**, *133*, 403–412; e) D. V. Kurandina, E. V. Eliseenkov, P. V. Ilyin, V. P. Boyarskiy, *Tetrahedron.* **2014**, *70*, 4043–4048; f) S. V. Kumar, D. W. Ma, *Chin. J. Chem.* **2018**, *36*, 1003–1006.

[15] M. Tian, X. L. Cui, M. Yuan, J. Yang, J. T. Ma, Z. P. Dong, *Green Chem.* **2017**, *19*, 1548–1554.

[16] The catalyst was prepared and characterized in our previously reported report: D. Z. Li, H. Lu, T. B. Yang, C. Xing, T. L. Sun, L. H. Fu, R. H. Qiu, *Catal. Commun.* **2022**, *162*, 106398.

[17] Deposition Number 2114849 (for **2a**) contains the supplementary crystallographic data for this paper. These data are provided free of charge by the joint Cambridge Crystallographic Data Centre and Fachinformationszentrum Karlsruhe Access Structures service.

[18] a) D. Poli, D. Catarzi, V. Colotta, F. Varano, G. Filacchioni, S. Daniele, L. Trincavelli, C. Martini, S. Paoletta, S. Moro, *J. Med. Chem.* **2011**, *54*, 2102–2113; b) S. Demirayak, C. Karaburun, R. Beis, *Eur. J. Med. Chem.* **2004**, *39*, 1089–1095; c) X. Cockcroft, K. J. Dillon, L. Dixon, J. Drzewiecki, F. Kerrigan, V. M. L. Loh, N. M. B. Martin, K. A. Menear, G. C. M. Smith, *Bioorg. Med. Chem. Lett.* **2006**, *16*, 1040–1044; d) B. L. Mylari, E. R. Larson, T. A. Beyer, W. J. Zembrowski, C. E. Aldinger, M. F. Dee, T. W. Siegel, D. H. Singleton, *J. Med. Chem.* **1991**, *34*, 108–122.

[19] a) R. Dopheide, L. Schroter, H. Zacharias, *Surf. Sci.* **1991**, *257*, 86–96; b) D. J. Alberas, J. Kiss, Z. M. Liu, J. M. White, *Surf. Sci.* **1992**, *278*, 51–61.

[20] K. S. Sanjay, X. Qiang, *Catal. Sci. Technol.* **2013**, *8*, 1889–1900.

[21] M. Lauwiner, R. Roth, P. Rys, *J. Appl. Cat. A.* **1999**, *177*, 9–14.